Monshausen et al
supplemental Figure 1

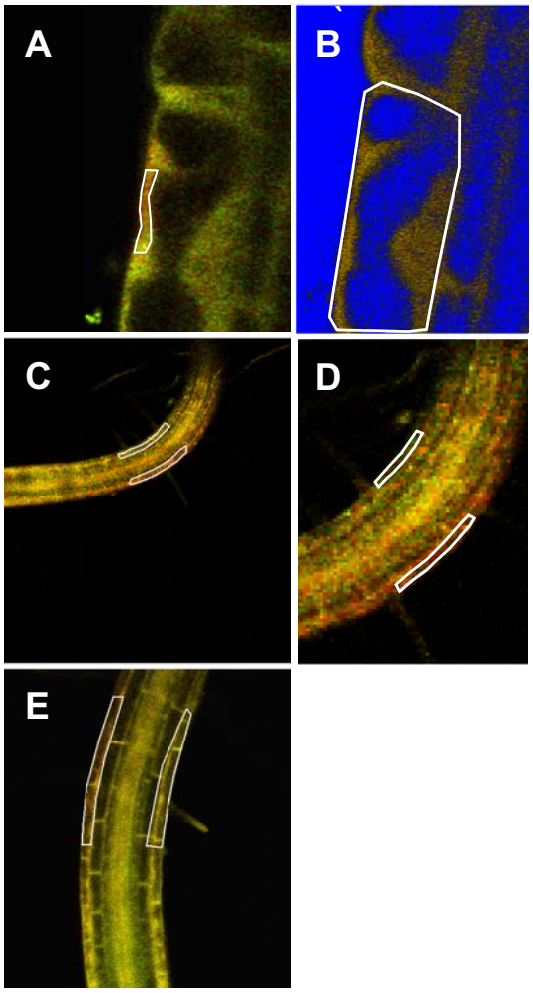

Supplemental Figure 1. Regions of interest (ROIs) selected for analysis of Ca^{2+}-dependent FRET/CFP ratios. The outlined ROIs correspond to those areas from which measurements were taken for (**A**) Figure 2A, (**B**) Figure 2A inset, (**C**) Figure 2B, (**D**) Figure 2B inset, and (**E**) Figure 2C. (**B**) Only areas not masked in blue were included in the analysis.

Monshausen et al
Supplemental Figure 2

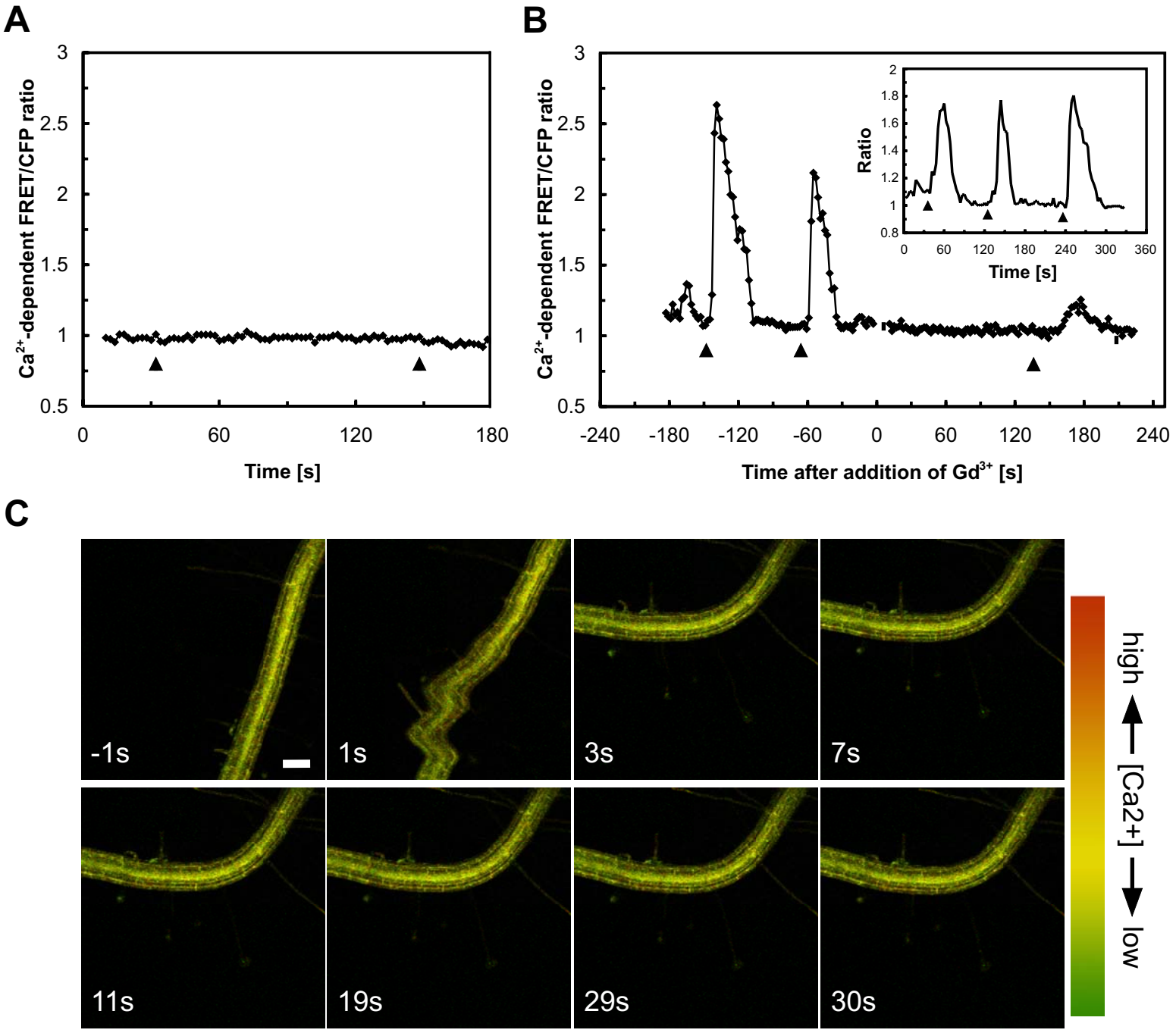

Supplemental Figure 2. Inhibition of mechanically induced cytosolic Ca^{2+} changes by Ca^{2+} channel blockers.
(**A**) Inhibition of touch-induced Ca^{2+} changes by pretreatment with 0.2 mM $LaCl_3$. Representative of n = 8 measurements. *Arrowheads*, touch stimulation.
(**B**) Inhibition of touch-induced Ca^{2+} changes by 1 mM $GdCl_3$. Touch-induced Ca^{2+} transients can be elicited even after multiple stimulations (*inset*); the strong attenuation of the Ca^{2+} signal after Gd^{3+} treatment thus reflects an inhibition rather than a desensitization of the response. Representative of n = 4 measurements. *Arrowheads*, touch stimulation.
(**C**) Inhibition of bending-induced Ca^{2+} changes by pretreatment with 1 mM $LaCl_3$. Representative of n = 7 measurements. Bar = 100 μm.

Monshausen et al
Supplemental Figure 3

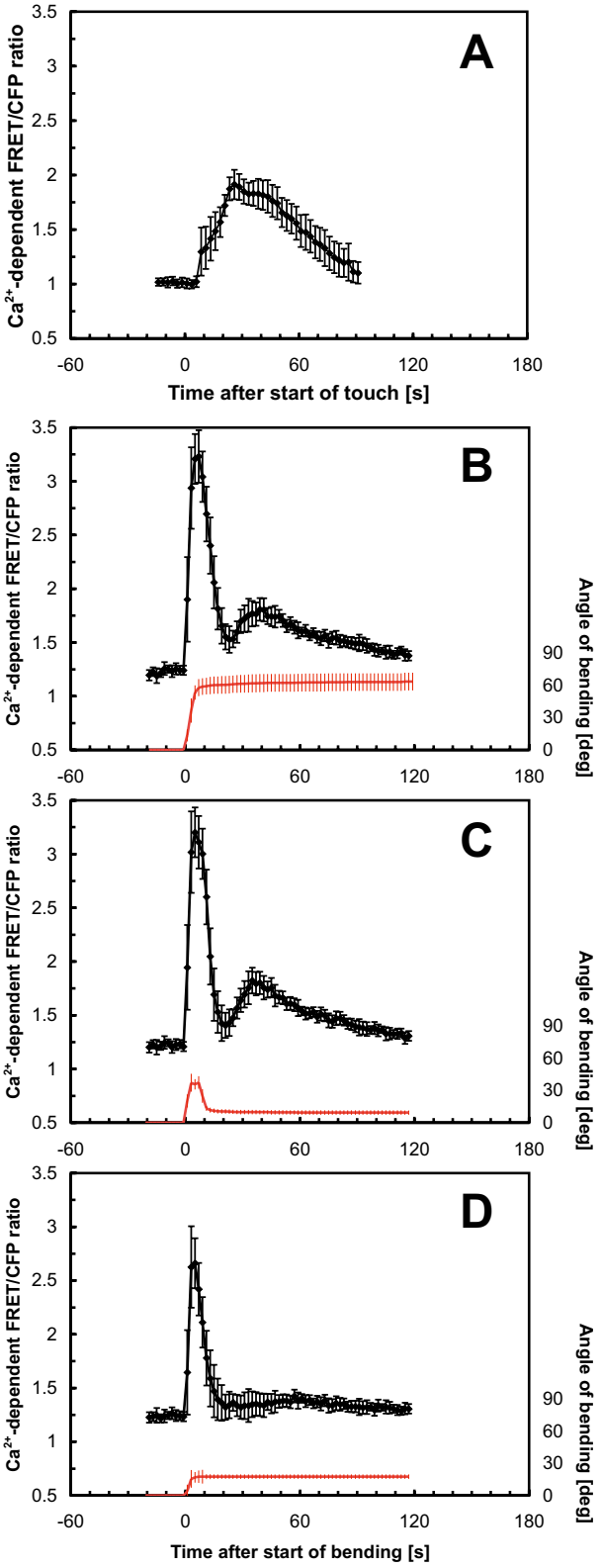

Supplemental Figure 3. Increase in cytosolic Ca^{2+} levels in response to root mechanical stimulation. Ca^{2+}-dependent FRET/CFP ratios were measured in ROIs close to the touch site as outlined in supplemental Figure S1A and C. An increase in ratio values indicates an increase in cytosolic Ca^{2+} levels.

(**A**) Monophasic Ca^{2+} changes in root epidermal cells in response to touch. The touch stimulus was applied for 27±15s (mean±SD). Note that even though the duration of the stimulus was variable, the Ca^{2+} response was very reproducible.

(**B-D**) Increase in cytosolic Ca^{2+} levels in response to root bending. The angle of the root tip relative to the root base is shown in red. Pre-stimulus angles are defined as 0 degrees.

(**B**) Biphasic Ca^{2+} changes on the convex side of bent roots in response to a sustained (>2 min) bending stimulus.

(**C**) Biphasic Ca^{2+} changes on the convex side of bent roots in response to a short (≤12s) bending stimulus.

(**D**) Ca^{2+} changes on the convex side of bent roots in response to a shallow (13-22º) bending stimulus. Note that the second peak at 60 s is strongly attenuated.

All values are means ± SE of n >= 4 experiments.

Monshausen et al
Supplemental Figure 4

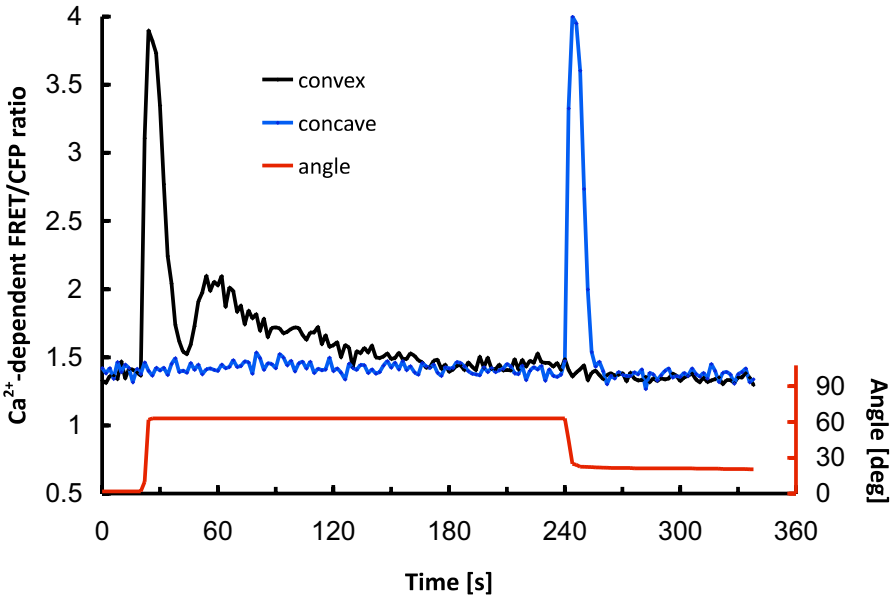

Supplemental Figure 4. During a bending stimulus, stretching and release of compression trigger Ca^{2+} signals with distinct signatures. Bending (at ca. 20s, *red curve*) elicits a biphasic Ca^{2+} response on the convex side of the root (*black curve*). Compression of cells on the concave side triggers either no detectable (*blue curve*) or a much lower monophasic Ca^{2+} elevation. Subsequent release of the bend (at ca. 240s, *red curve*) is not accompanied by Ca^{2+} changes on the former convex side, but the release of sustained compression on the former concave side results in a strong and consistently monophasic Ca^{2+} increase.

Monshausen et al
Supplemental
Figure 5

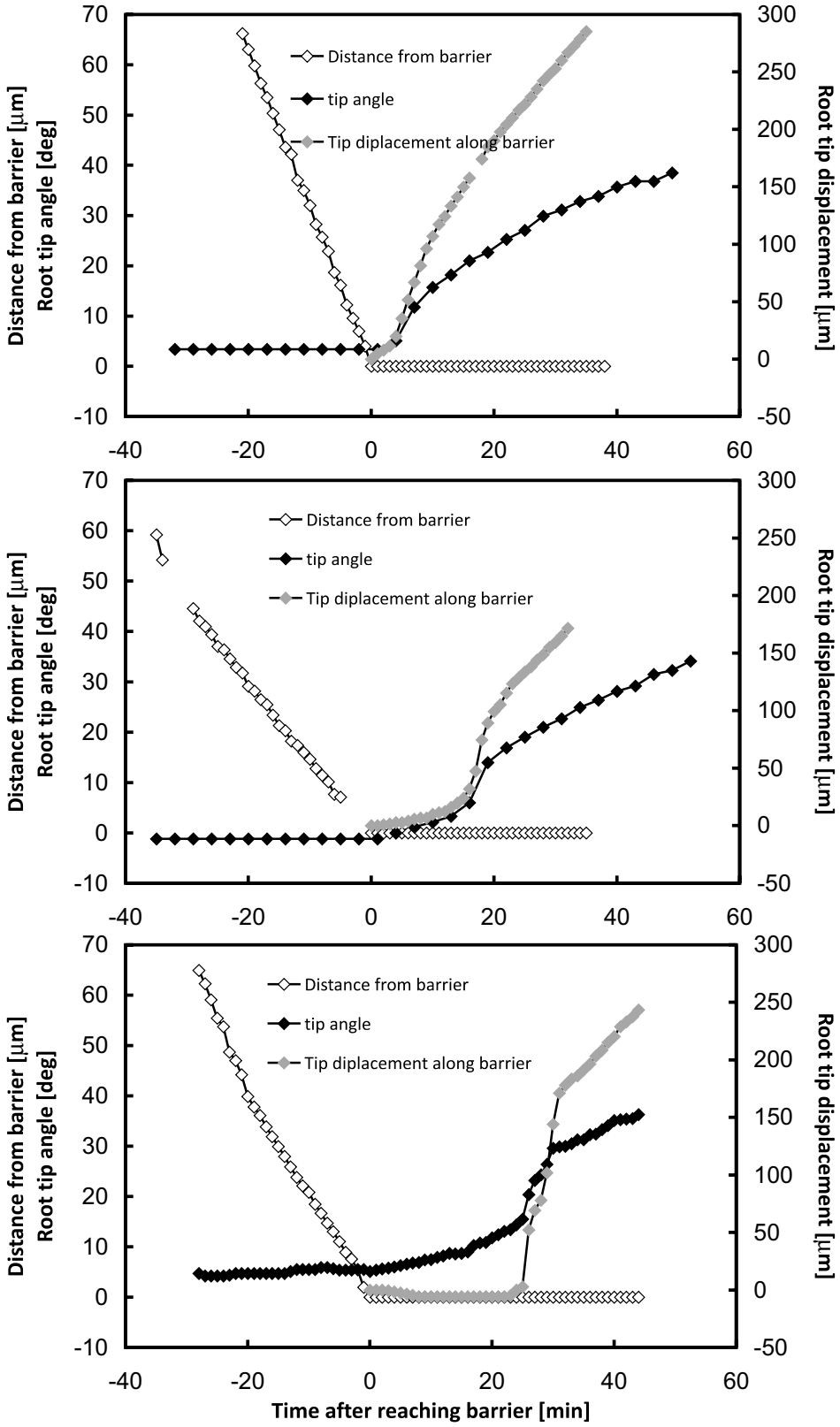

Supplemental Figure 5. Three examples of *Arabidopsis* roots showing the range of characteristic thigmotropic growth responses upon encountering an impenetrable barrier. Roots were grown in agarose on the vertical stage of a Nikon Diaphot TE300 microscope (Nikon, Melville, NY). The barrier consisted of a piece of coverglass inserted into the agarose perpendicular to the root growth direction. Root growth was monitored by acquiring images every 30s. *Open diamonds*, distance of the extreme root tip from the coverglass barrier. As the root tip approaches the barrier, the distance decreases. Once the root tip contacts the barrier at time 0s, the contact is maintained and the distance remains 0 μm. *Black diamonds*, root angle. The root tip approaches the barrier at a fairly constant angle (between -1 and 5º for the shown measurements). As the roots encounter the barrier, the position of the root tips initially changes very little as the roots press against the obstacle. This is followed by a sudden 'slippage' of the root tip to the side (after 4-25 min for the shown measurements), producing a bend in the basal elongation zone. *Gray diamonds*, root tip displacement along the barrier. Note the sudden increase in displacement as the root angle increases, indicating root tip slippage.

Monshausen et al
Supplemental Figure 6

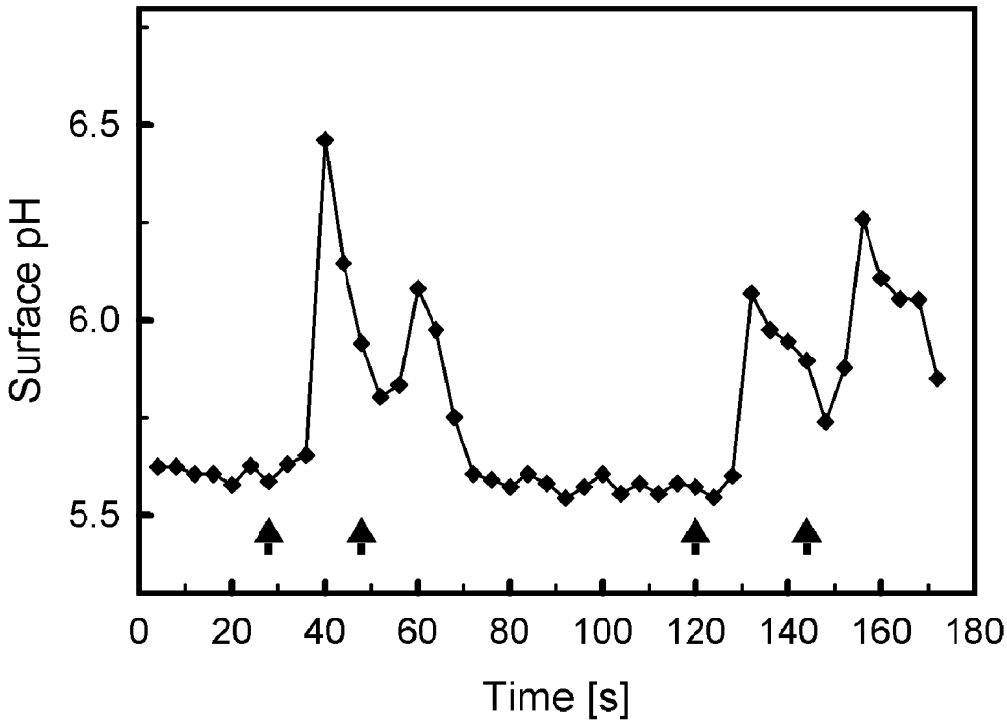

Supplemental Figure 6. Measurement of cell surface pH changes during repeated touch stimulation. No clear refractory period for this response was observed down to 20-s intervals between stimuli, which represented the minimum interval for a touch-induced extracellular pH change to show a clear falling phase once it was triggered.

Monshausen et al
Supplemental Figure 7

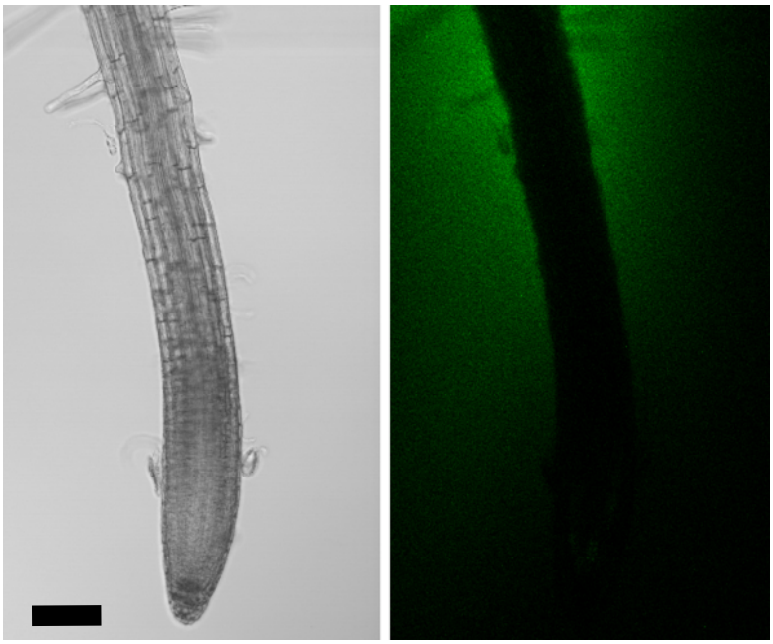

Supplemental Figure 7. ROS-dependent OxyBURST fluorescence pattern around growing *Arabidopsis* root. At the time of image acquisition, the root had been incubated in OxyBURST for 1 min. Note that ROS production is strongest in the proximal elongation and root hair zone of the root. Bar = 100 μm.

Monshausen et al,
Supplemental Figure 8

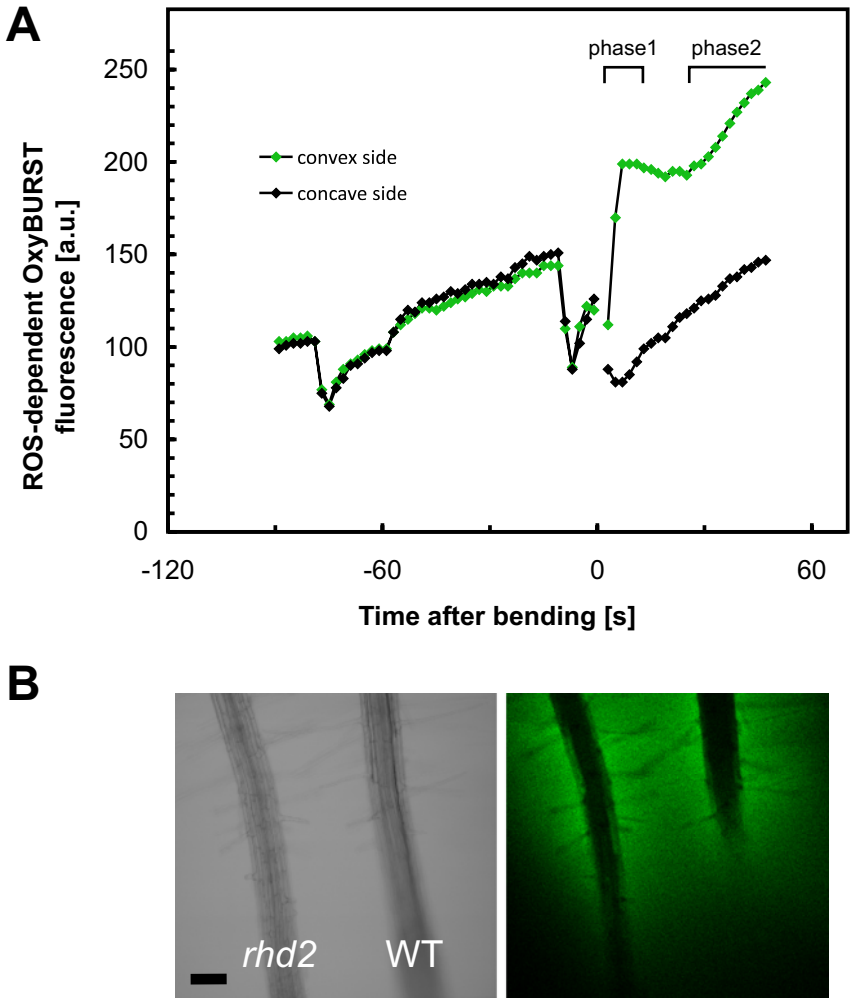

Supplemental Figure 8. Extracellular ROS pattern around roots of *rhd2*. (**A**) Effect of bending on extracellular ROS production of *rhd2* root. ROS-dependent accumulation of OxyBURST fluorescence was monitored at the root surface. At -78s, the medium was gently mixed by pipetting to dissipate the fluorescence gradient around the root. The medium was mixed again at -11s after which the root was bent (0s). Note the strong increase in fluorescence asymmetry after the bending stimulus, indicating enhanced biphasic ROS production on the convex side of the root. (**B**) ROS-dependent OxyBURST fluorescence pattern around *rhd2* and WT roots. The root hair phenotype of *rhd2* was rescued by growing roots at elevated pH (Monshausen et al., 2007). Note the similar ROS patterns of WT and *rhd2* roots growing side by side. Bar = 100 µm.

Monshausen et al
Supplemental Figure 9

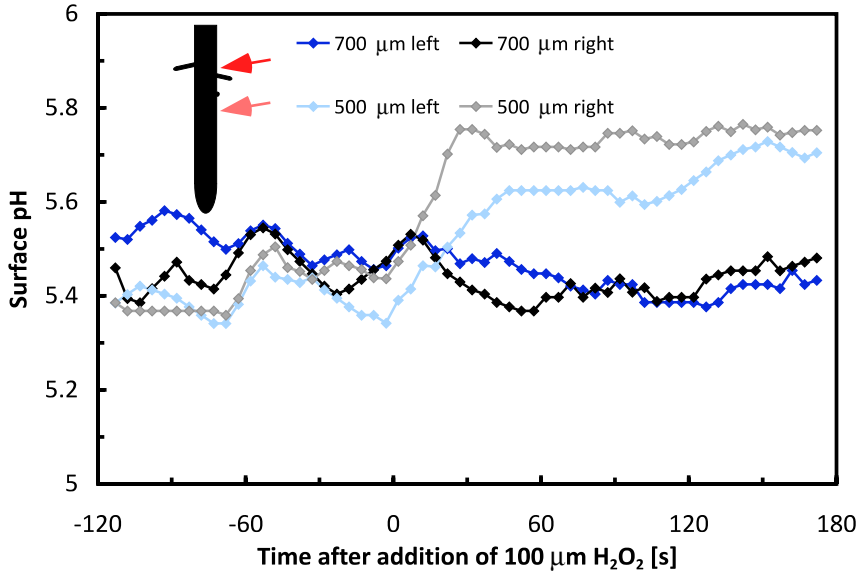

Supplemental Figure 9. Effect of exogenous ROS on root surface pH. Treatment of Arabidopsis roots with as much as 100 µM H_2O_2 did not affect root surface pH in the mature zone (700 µm from apex) within the first 3 min of treatment, indicating that rapid pH changes monitored in this zone during touch and bending (Figures 3 and 4) are independent of concomitant ROS production. However, longer exposure to 100 µM H_2O_2 (but not 10 µM H_2O_2, data not shown) resulted in a weak alkalinization in this zone. More apical regions of the root (e.g. at 500 µm) responded to the treatment with a clear surface alkalinization, indicating tissue-specific sensitivity to exogenous ROS. Surface pH was monitored in ROIs at 700 µm (*dark blue, black*) and 500 µm (*light blue, grey*) distance from the root tip on the left side (*dark blue, light blue*) and right side (*black, grey*) of the root. Arrows indicate the approximate position of the ROIs analyzed.

Monshausen et al
Supplemental Figure 10

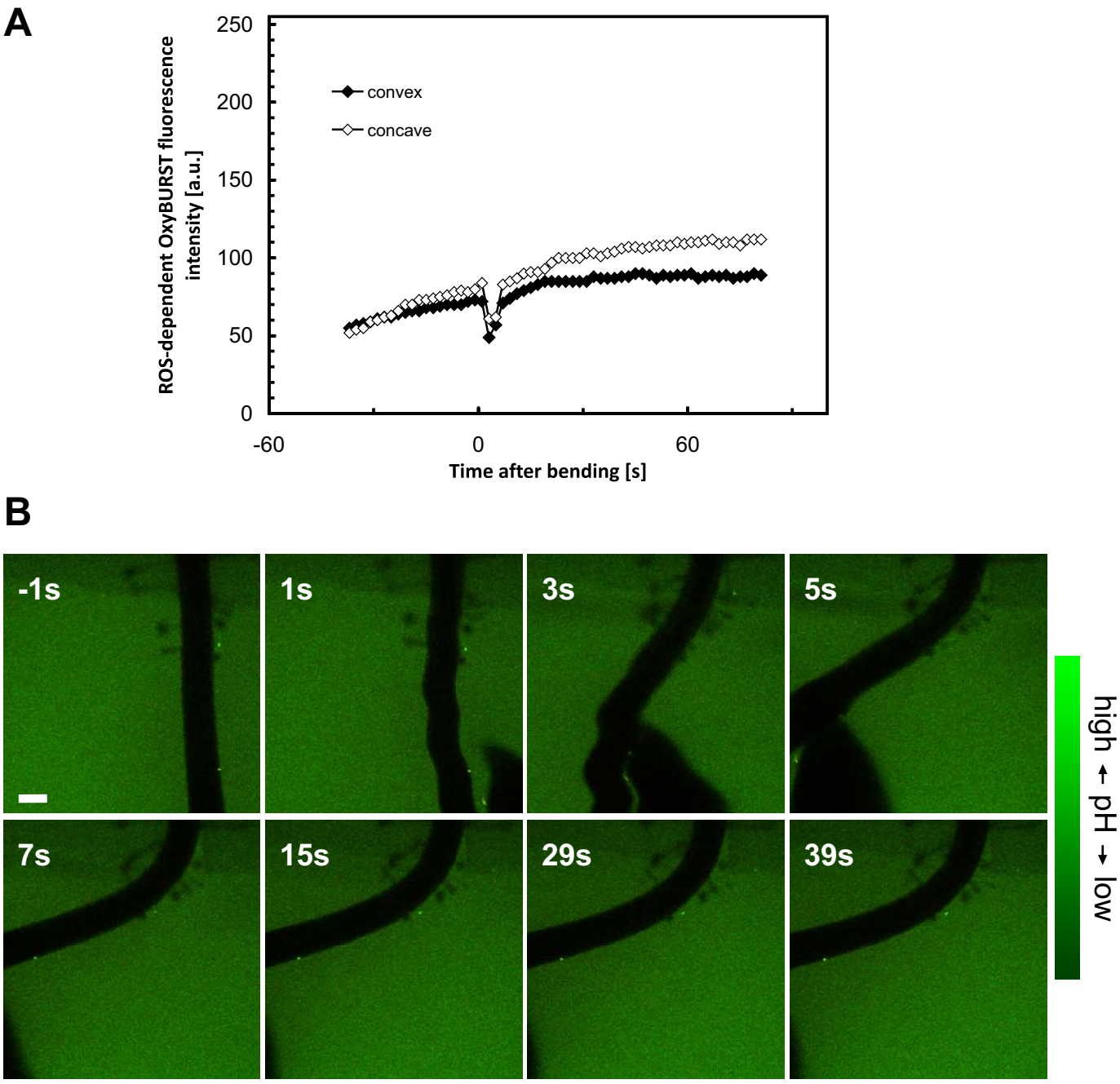

Supplemental Figure 10. Effect of the Ca^{2+} channel inhibitor La^{3+} on bending-induced ROS and pH changes.

(**A**) Inhibition of ROS production during root bending by La^{3+}. The root was pre-incubated with 1 mM $LaCl_3$ for 3 min prior to bending. ROS production was determined by monitoring OxyBURST fluorescence.

(**B**) Inhibition of surface pH changes during root bending by La^{3+}. The root was pre-incubated with 1 mM $LaCl_3$ for 3 min prior to bending. pH was determined by monitoring fluorescein fluorescence.

Monshausen et al
Supplemental Figure 11

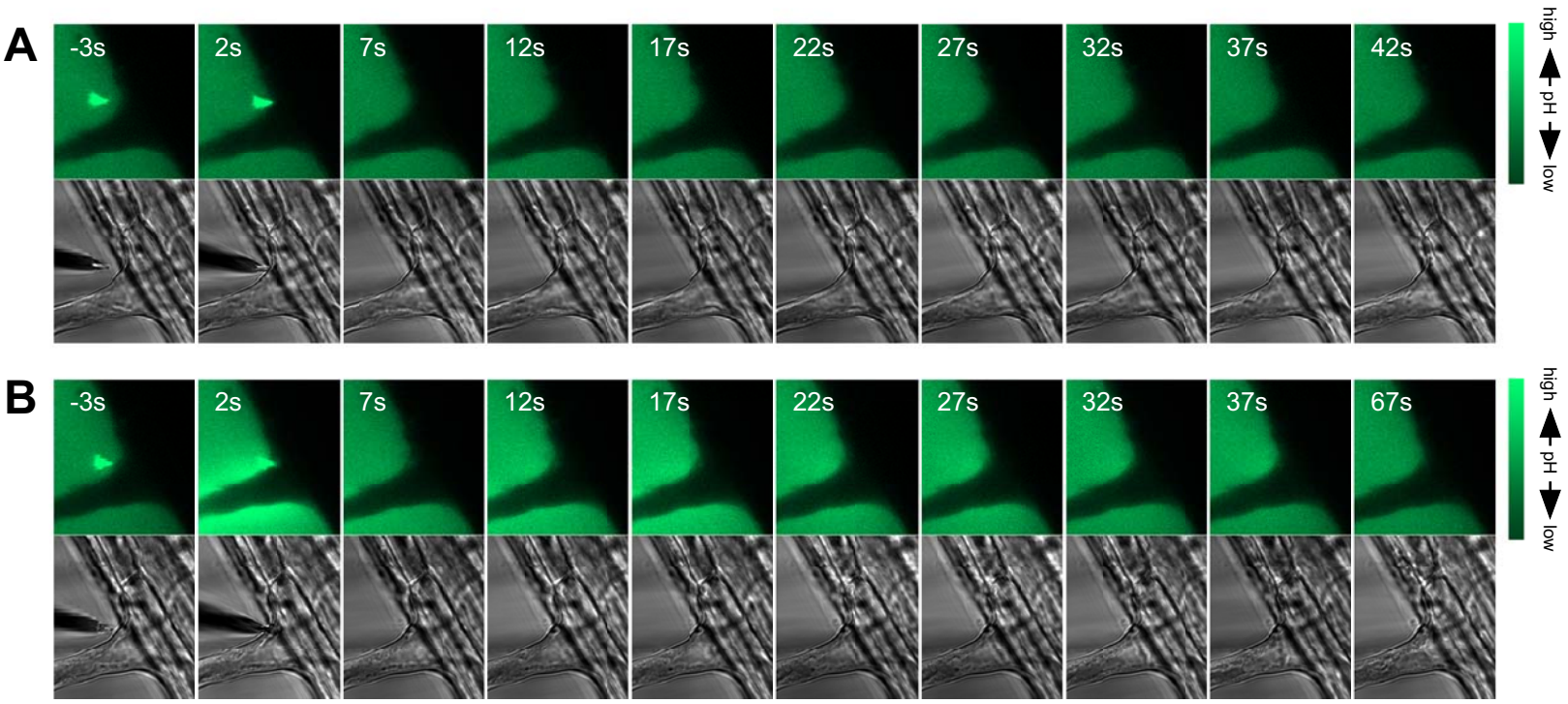

Supplemental Figure 11. Inhibition of touch-induced surface pH changes by La^{3+}.
(**A**) Pre-incubation with 100 µM $LaCl_3$ inhibited touch-induced cell surface alkalinization. Numbers represent time after the start of the touch stimulus in seconds. Bar = 10 µm.
(**B**) Pre-incubation with 100 µM $LaCl_3$ did not inhibit cell surface alkalinization triggered by wounding the same cell, indicating that La^{3+} does not interfere with the cell's capacity to alter its surface pH but rather blocks the channel-mediated Ca^{2+} influx required to trigger the pH response. Numbers represent time after the start of wounding in seconds. Note the wound site is visible in bright field images from 7s onward.